



Geophysical Well Log Appraisal of Okpella Field within Offshore Niger Delta Basin of Nigeria

**E. U. Waziri ^{a*}, E. E. Udensi ^a, C. I. Unuevho ^a, M. O. Jimoh ^a, U. D. Alhassan ^a,
K. A. Salako ^a and A. A. Solomon ^b**

^a Department of Physics, Federal University of Technology, Minna, Niger State, Nigeria.
^b Department of Geosciences, University of Lagos, Nigeria.

Authors' contributions

This work was carried out in collaboration among all authors. All authors read and approved the final manuscript.

Article Information

DOI: 10.9734/JGEESI/2022/v26i530350

Open Peer Review History:

This journal follows the Advanced Open Peer Review policy. Identity of the Reviewers, Editor(s) and additional Reviewers, peer review comments, different versions of the manuscript, comments of the editors, etc are available here: <https://www.sdiarticle5.com/review-history/84946>

Original Research Article

**Received 20 January 2022
Accepted 24 March 2022
Published 18 May 2022**

ABSTRACT

The Production data of Okpella Field, located within the Offshore Niger Delta Basin, Nigeria, revealed that the Okpella Field attained peak annual hydrocarbon production of 430175 MBO (Million Barrel of Oil) in 2008, and the production has presently dropped to 7839 MBO per annum. Therefore, an appraisal study was conducted to identify opportunities for reversing the low production. The sought opportunities were bypassed reservoirs with pay zones. This study uses geophysical Well log data, Biostratigraphic data, and Production data to appraise Okpella Field. The hydrocarbon production data were analyzed for the produced reservoirs to establish the positive effects of the Bypassed hydrocarbon reservoirs zone within Okpella Field Offshore Niger Delta Basin. Before this study, the operating company had previously identified six reservoirs. They were named major reservoirs Sand A to F, of which major reservoirs B, C, and E are gas-bearing, major reservoir D bears gas and oil, and major reservoir F bears condensates. Three additional reservoirs with pay zones were identified within this study, and they were named Bypassed A to C. Bypassed A is gas bearing, Bypassed B is oil and gas and Bypassed C is oil-bearing. The petrophysical analysis of the wells within Okpella Field determined the various reservoir properties such as the gross thickness, net thickness, net to gross ratio, the volume of shale, porosity, and hydrocarbon saturation of the major reservoir and bypassed reservoir zones. Some of the reservoirs are amalgamated upward coarsening sand bodies of distal fan lobes within the Low-stand systems

*Corresponding author: E-mail: uduagbami2090@gmail.com;

tract. Others are leveed channel proximal. The Biostratigraphy data were integrated with the stacking pattern of the Gamma-ray log motif, revealing the sequence boundaries and inferring the possible depositional environment. The reservoirs within the Okpella Field were deposited within the Low-Stand System Tract (LST), reflecting a high energy environment, possibly the shoreface depositional environment.

Keywords: Major reservoir; bypassed reservoir; net pay; hydrocarbon saturation; fluid types.

1. INTRODUCTION

Basins are crustal depressions on the earth's surface within which sediments accumulate and lithify to form sedimentary rocks. Bypassed hydrocarbon constitutes opportunities for sustaining production and increasing recovery in mature Field [1]. In a mature field with a large number of wells and production information, the undrilled areas between wells (or inter-well areas) constitute areas of geologic uncertainty that may enhance production significantly [2]. Okpella Field attained peak production in 2008 and is now mature with relatively low hydrocarbon recovery. Like all Niger Delta wells, its wells are multi-reservoir wells with chances of having unproduced reservoirs with pay zones. Opportunities for reversing the present low hydrocarbon recovery in the Field involve identifying unproduced reservoirs with pay zones. This requires a re-evaluation of the Field using cutting-edge software supported petrophysical analysis hinged on sequence stratigraphic techniques. The essential purpose of Well log analysis is to derive the petrophysical properties of reservoirs such as porosity, shale volume, hydrocarbon saturation, net pay thickness, net to gross for hydrocarbon exploration Ahmed et al. [3].

The productivity of wells in hydrocarbon-bearing reservoirs relies on petrophysical properties, such as lithology, porosity, water saturation, and permeability [4]. Shale volume (V_{CL}), porosity (Φ), water saturation (S_w), hydrocarbon saturation (S_h), gross reservoir thickness, and net pay thickness are the petrophysical properties estimated for each identified reservoir within the Wells.

The two major lithologic units within the Niger-Delta basin are Sand and Shale, as revealed by formation evaluation and reservoir characterization of some parts of the Niger-Delta [5]. A good reservoir is commercially productive if enough oil or gas can be produced to pay back its investors for the drilling cost and leaves a profit [6].

Several authors have carried out Well Log Aprasials on different fields within different sedimentary basins worldwide; for instance, Mohamed et al. [7] Carried out well-logging data interpretation to appraise Alam El-Bueib reservoir's performance in Safir Oil Field, Shushan Basin, Egypt. Ahmed et al. [3] identified and characterized the main reservoirs of Al Baraka Oil Field in Komobo Basin, Upper Egypt, using petrophysical analysis of Well log data. Rotimi et al. [8] carried out a Petrophysical analysis and Sequence Stratigraphy of Well Log data to appraise Bobo Field, South-Eastern, Niger Delta.

The central focus of this study is to develop a framework for reversing the present low hydrocarbon recovery trend in Okpella Field by re-evaluating the Field using Well Log Data to identify reservoirs with pay zone, delineate bypassed hydrocarbon reservoirs, and analyze the petrophysical properties of the identified reservoirs.

2. LOCATION OF THE STUDY AREA

Okpella Field is situated on the continental margin of the Gulf of Guinea in equatorial West Africa at the southern end of Nigeria bordering the Atlantic Ocean, between latitudes $5^{\circ} 52'50''$ and $6^{\circ} 15' 00''$ and longitudes $4^{\circ} 81'25''$ and $4^{\circ} 92'25''$ (Fig.1). The Niger Delta covers a 75,000 square kilometres area with a clastic fill of about 12 000m within the Gulf of Guinea, West Africa [9]. The Niger Delta is bounded to the north by the Anambra Basin, to the west by the Okitipupa High, the Benin Flank, and the east by the volcanic rocks of the Cameroon volcanic zone. The location of the study area and base map of the Okpella field showing the well location is presented in (Figs.1 and 2).

2.1 Regional Geology of the Niger Delta Basin

The Niger Delta is part of the world's prolific deltaic systems. The delta covers an

approximate area of about 300,000 km² [10], with a sediment volume of 500,000 km³ [11] and sediment thickness ranging between 9,000 and 12,000 m. The modern Niger Delta is formed in the Early Tertiary, sediments accumulated in this region during the Mesozoic rifting, between Africa and South American continents [12,13,14] Major submarine canyons delivered sediments from the shelf edge into the marine environment.

Some canyons are Lagos, Avon, Mahin in the west, Niger canyon at the centre, and Kwa Ibo and Calabar in the east. The delta extends more than 300 km from apex to mouth [14]. It forms one of the world's primary hydrocarbon provinces, with proven ultimate recoverable reserves of approximately 26 billion barrels of oil and an evaluated but probably vast gas resource base [14].

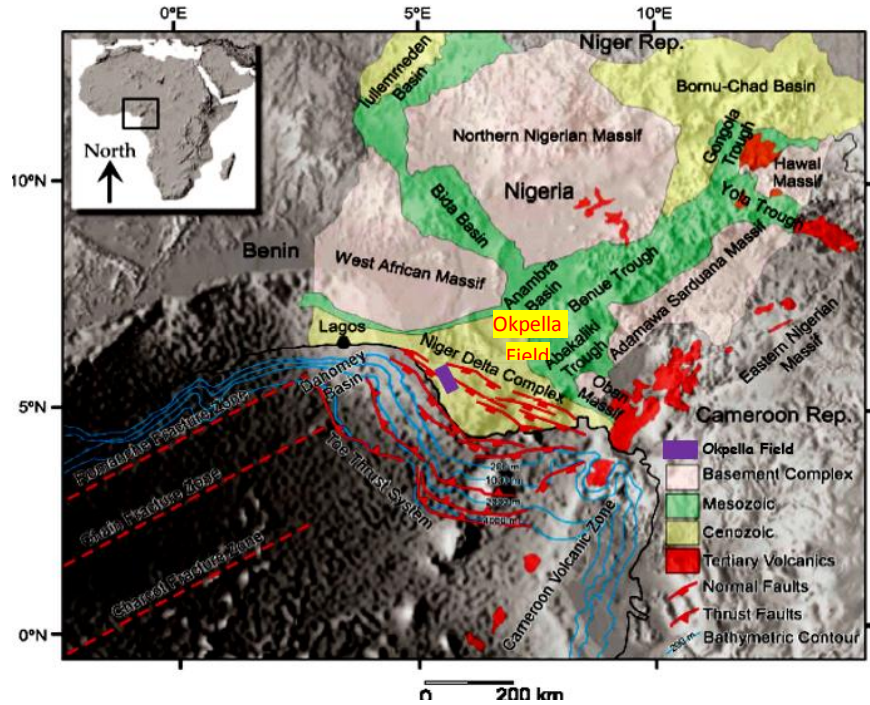


Fig. 1. Geological Map of Nigeria showing the Niger Delta basin and location of Okpella Field

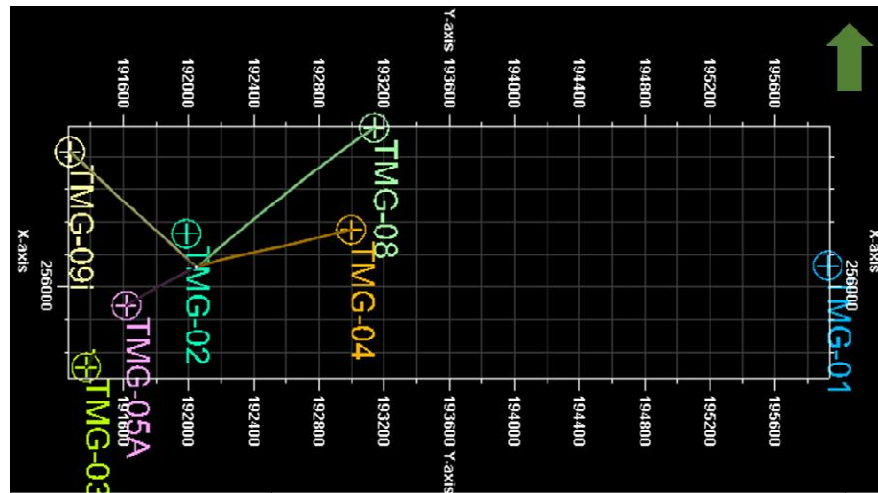


Fig. 2. Base Map of Okpella Field showing well location

The evolution of the Niger Delta is closely tied to the origin of the Benue trough in the late cretaceous [9]. The breakup of the Central Africa-South America part of Gondwanaland took place in the Mesozoic along a series of rift zones of different orientations that met in a triple junction in the present Gulf of Guinea position now occupied by the Niger delta. Two of the arms, which followed the south-western and south-eastern coasts of Nigeria and Cameroon, developed into collapsed continental margins of the South Atlantic. In contrast, the third failed arm extended into the Benue Trough, as shown in (Fig. 3). [14]. The primary depocentre is thought to have been at the triple junction between the continental and oceanic crust, where the delta reached a primary zone of crustal instability. The Niger Delta is a sizeable arcuate delta of the destructive, wave-dominated type. It is composed of a regressive clastic sequence that reaches a maximum thickness of about 12 km in the basin centre.

The main Formations that have been recognized in the subsurface of the Niger Delta are Benin, Agbada, and Akata Formations (Fig. 4). These Formations were deposited in continental, transitional, and marine environments, respectively; together, they form a thick, overall progradational passive-margin wedge [9]. The

Akata Formation is the basal unit composed mainly of marine shales believed to be the primary source rock within the basin.

The Akata Formation occurs as deltaic dark grey shales and silts with occasional thin sands of likely turbidite flow origin. It is estimated to be about 6,400m thick in the central part. The marine Planktonic Foraminifera suggests a shallow marine shelf depositional setting ranging from Paleocene to recent age [16, 17].

Agbada Formation consists of alternating sands, silts, and shales, defined by progressively upward grain size and bed thickness alteration. The strata are known to have formed in fluvio-deltaic environments. The Formation age is from Eocene to the Pleistocene. The youngest marine shale defines the base, and the top is characterized by a subaerially exposed delta surface, which extends to about 4600 feet in depth. Shallow parts of the formation are composed entirely of non-marine Sand deposited in alluvial or upper coastal plain environments during the progradation of the delta [16]. Although lack of preserved fauna inhibits accurate age dating, the age of the formation is estimated to range from Oligocene to Recent [18].

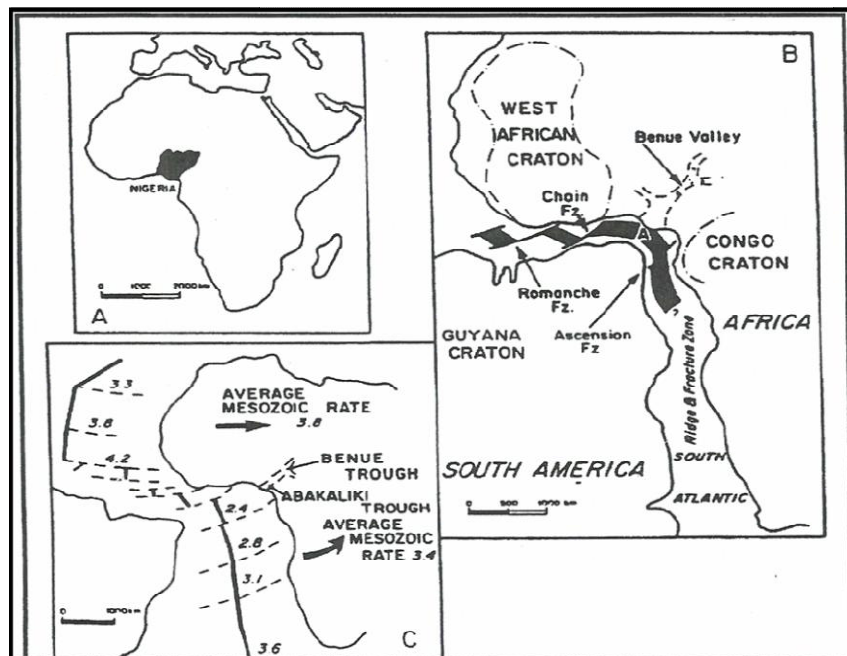


Fig. 3. (a) Location of Nigeria (B) Early cretaceous separation of Africa and South America (C) Mesozoic seafloor spreading for Africa and South America after [15]

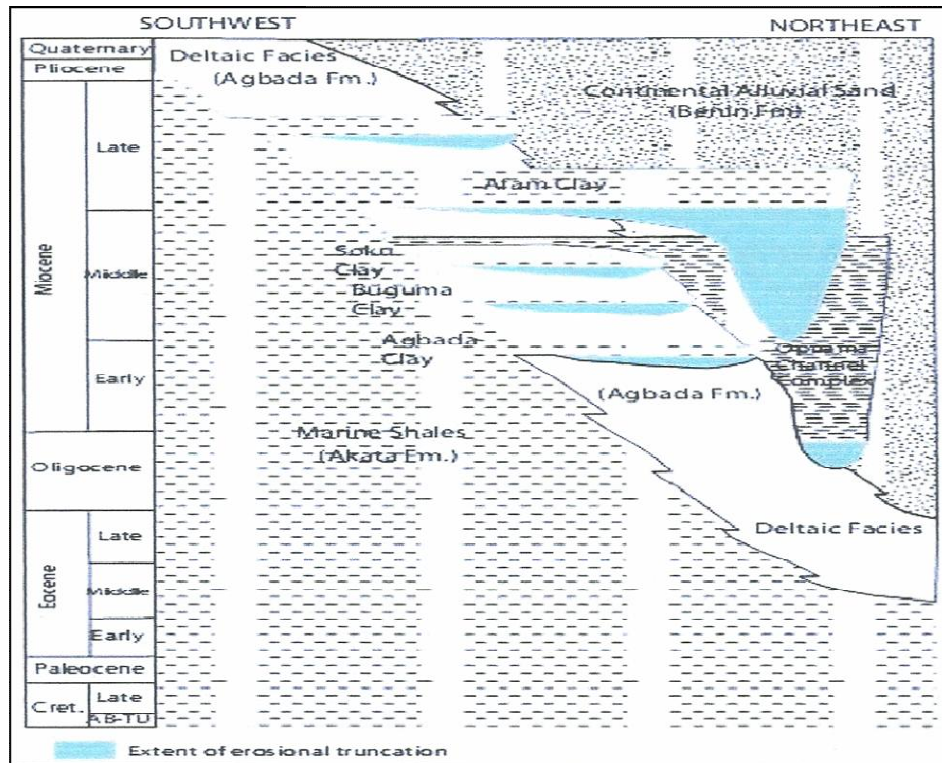


Fig. 4. Stratigraphic column of the Niger Delta showing the three Formations (Modified from Shannon and Naylor [15])

The Benin Formation has a high sand percentage of about 70–100% and forms the top layer of the Niger Delta depositional sequence. The massive sands were deposited in continental environments comprising the upper delta plain’s fluvial realms (braided and meandering systems). The oldest continental sands are probably Oligocene, although they lack fauna and are impossible to date directly. Offshore, they become thinner and disappear near the shelf edge [14].

3. MATERIALS AND METHODS

The data used for this study are geophysical composite logs, well deviations, and stratigraphic sequence tops. These data were obtained from the operating company with the permission of the Department of Petroleum Resources Nigeria. The geophysical composite logs comprise of Gamma-ray (GR), Resistivity log (LLD), Neutron log, Density log, and Sonic Log. The software used for the Petrophysical analysis is the student version of the Synergy Interactive Petrophysics (IP) software, and the software used for the Reservoir correlation is the Schlumberger Petrel.

3.1 Depositional Environment

Sequence boundaries were defined by looking for abrupt bases of low-gamma ray-value intervals on the Well logs because abrupt changes in gamma-ray logs response are commonly related to sharp lithological breaks [19]. The stratigraphic sequence tops were delineated from foraminiferal contents, comprised of benthic and planktonic forams. The stratigraphic tops were integrated with the log motifs of the Gamma-ray (Fig.5) [20] to reconstruct the possible depositional environments, develop a lithofacies model for each well, and delineate Sequence Stratigraphic Surfaces such as Sequence Boundary, Flooding surfaces, and Maximum Flooding Surfaces. Stratigraphic sequence can be sub-divided into smaller sediment packages called systems tracts based on characteristic well-log patterns [21].

The volume of Shale Computation (Vsh): Sandstone units were differentiated from shale units using the gamma-ray log and Neutron/Density logs [22]. The GR value for clean Sand and shale was chosen using a Gr histogram distribution (Fig.6). A maximum GR

value of 60 API was selected as the cut-off of sandstone units. Gamma-Ray Index was estimated for each reservoir using equation 1.

$$I_{GR} = \frac{GR - GR_{CN}}{GR_{SH} - GR_{CN}} \quad (1)$$

where GR is gamma-ray log reading in the reservoir of interest, GR_{CN} is gamma-ray log response in clean (shale free) Sand, and

GR_{SH} is the highest gamma-ray reading for shale.

The estimated Gamma-Ray index was utilized to estimate shale volume (V_{SH}) [23] Islam et al. [24] for each reservoir using equation 2, Larionov V_{SH} estimation equation for Tertiary rocks:

$$V_{SH} = 0.083(2^{3.7 * I_{GR}} - 1) \quad (2)$$

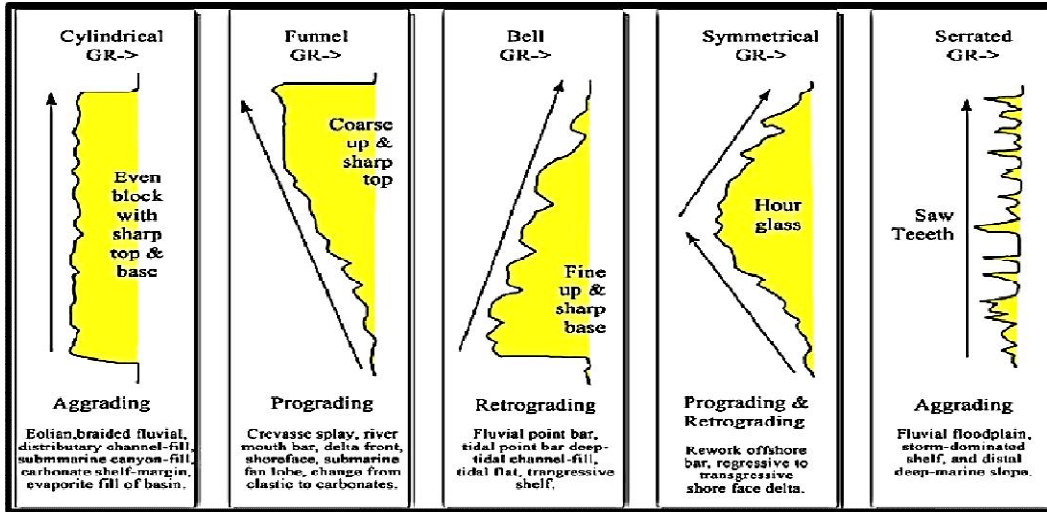


Fig. 5. Gamma-ray motif character for the different depositional environments after [20]

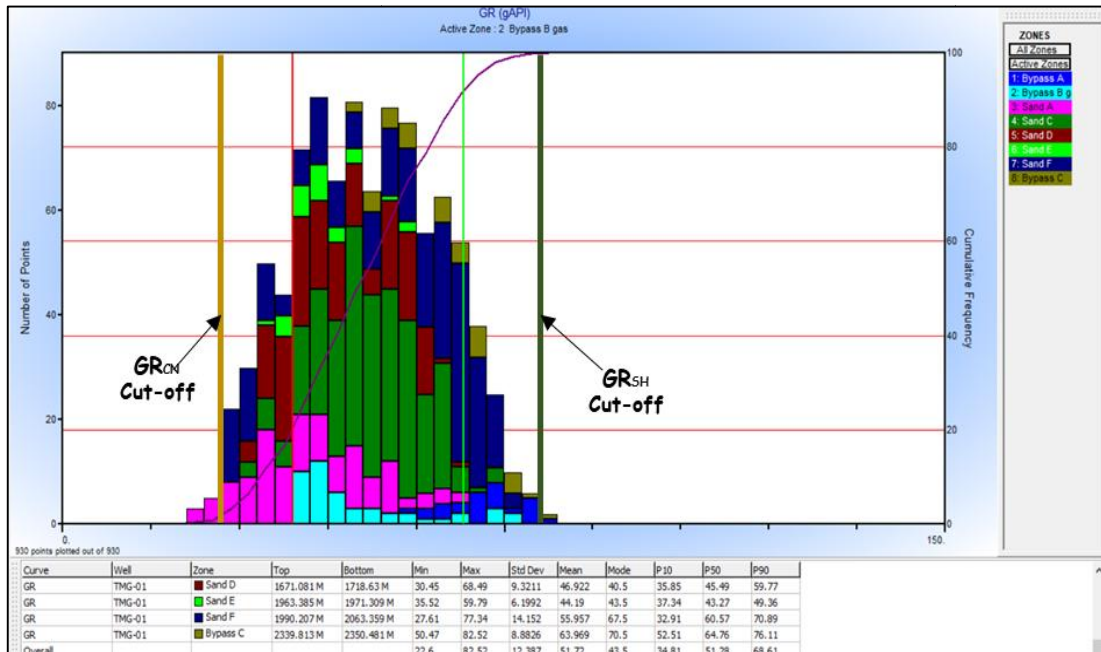


Fig. 6. Histogram plot of Gr for estimating cut off

Porosity Computation: The porosity Φ was estimated from density logs using equation 3, where P_{ma} (2.65g/cm^3) is the bulk density of sand matrix, P_b is reservoir bulk density obtained from bulk density log, and P_f is the density of fluid derived from the Neutron/Density cross plot [25].

$$\Phi = \frac{P_{ma} - P_b}{P_{ma} - P_f} \quad (3)$$

Gross and Net thickness of the reservoir: The Gross thickness was derived by subtracting the top and base of each reservoir unit. The net thickness was derived by eliminating the shale thickness that adds to the gross thickness. The Net to Gross ratio is the percentage ratio of the net Sand to the total or gross reservoir sand Nwankwo et al. [26].

Water Saturation Computation: Water saturation (S_w) was estimated using Archie's method in equation 4 [27]. Water Resistivity (R_w), Porosity (Φ), tortuosity factor (a) of 1, saturation exponent (n) of 2, and cementation exponent (m) of 1 [27]. The Water resistivity was derived using the Pickett plot in reservoirs wholly saturated with water (Fig.7), [28]. The hydrocarbon saturation was estimated from the water saturation using equation 5.

$$S_w = \left(\frac{a R_w}{R_t \Phi^m} \right)^{\frac{1}{n}} \quad (4)$$

$$S_h = 1 - S_w \quad (5)$$

Fluid Identification: Sand units with anomalously high resistivity values were identified as hydrocarbon reservoirs. Fluid types (gas, oil, and Water) and fluid contacts (gas oil contact (GOC) and oil water contact (OWC)) within the reservoirs were identified by the integration of Resistivity and Neutron/Density logs [29]. Resistivity logs identified oil-water contacts, while Gas oil contact was identified by Neutron/Density cross plot (Fig.8). Significant separation within the neutron and density curve when the resistivity curve (balloon effect) indicates gas, while low separation indicates oil [30]. The lowest known Gas and oil contacts were taken as the gas contact or oil contact.

Reservoir Sums and Averages: The petrophysical properties curves were generated based on the composite logs, such as volume of shales (Vsh), porosity (Φ), and water saturation (S_w). The cut-off values adopted in this study for the derived petrophysical properties are 0.5 for

the volume of shale, 0.1 for porosity, and 0.7 for water saturation of 0.7.

4. RESULTS AND DISCUSSION

4.1 Reservoir Correlation

The reservoirs identified by the operating company are the major hydrocarbon reservoirs in this study. Some hydrocarbon reservoirs were unidentified in-house by the operating company but were identified in this study, called bypassed hydrocarbon reservoirs. They are strictly reservoirs with pay zones penetrating the wells but bypassed reservoirs in unperforated areas. For simplicity, they are bypassed in the wells as they contain unproduced hydrocarbons at the end of conventional recovery exercise. Bypass B was correlated across TMG-01, TMG-08, TMG-05A, TMG-03 and TMG-09i. Bypass C is only present in TMG-01 at a deeper depth. Sand B and Sand C are absent in TMG 01 but found in all the wells on the downthrown fault block, (Fig.9). This is probably due to disruption in lateral facies continuity due to faulting.

4.2 Environment of Deposition (EOD)

The sequence stratigraphic surfaces, which are the sequence boundaries (SB) and maximum flooding surfaces (MFS), were derived from the biostratigraphic data. These surfaces were identified and correlated across the wells. At the same time, the environment of deposition of the reservoirs was identified using the gamma-ray log motif.

Three depositional sequences were delineated in wells TMG 08, TMG 04, and TMG 9i. TMG 02, the deepest well, has six delineated depositional sequences. Four depositional sequences were delineated in TMG 05A and TMG 03. The major hydrocarbon reservoirs and bypassed reservoirs are associated with the low-stand systems tract. Hydrocarbon reservoirs Sand B and Sand C are amalgamated upward coarsening sand bodies in wells TMG 08, TMG 04, TMG 02, TMG 5A, and TMG 9i. They are distal fan lobes prograding over basal shales. The LST sand bodies in wells TMG 02 (Sand D, Sand E, and Sand F) in TMG 5A (Sand D) and TMG 03(Sand D) are upward fining. These are leveed channel proximal fans deposited over bathyal shales. (Fig.10) is the correlated sequence stratigraphic framework for the wells in Okpella Field.

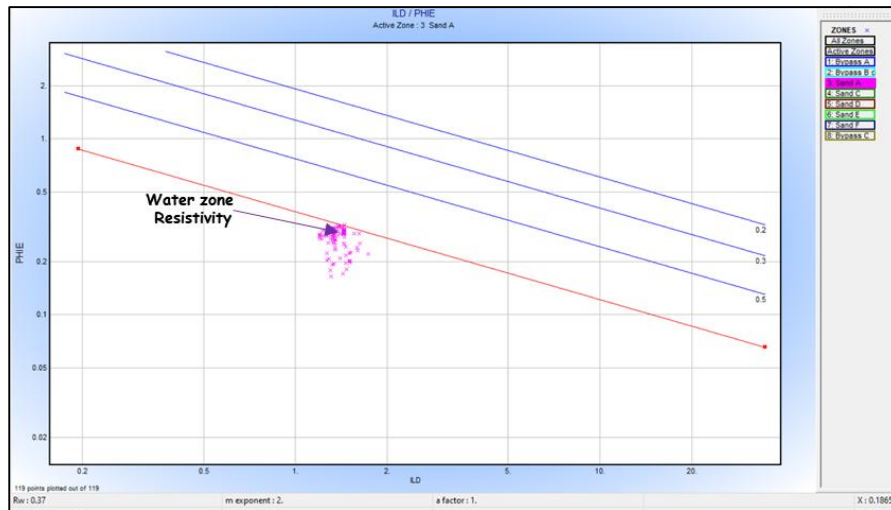


Fig. 7. R_w estimation using Pickett plot for a zone that is completely saturated with water

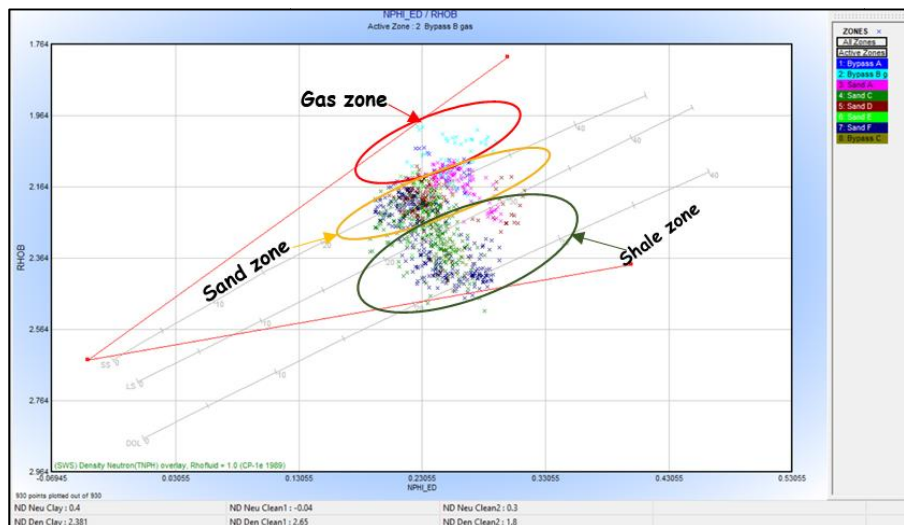


Fig. 8. Complex cross plot of neutron and density log in which the red circle shows the gas zones

4.3 Reservoir Fluid Type Analysis

It is known that not all the correlated reservoirs contain hydrocarbons in the basin or Field. The reservoirs in this study containing hydrocarbons were identified using the resistivity log. The hydrocarbons in these reservoirs could be oil or gas. The reservoirs with high resistivity values indicate the presence of hydrocarbon. In contrast, reservoirs with low resistivity values indicate the presence of water.

Bypassed reservoirs A are gas reservoirs in TMG-01 and TMG-05A (Fig.11). In contrast,

bypassed reservoir B is an oil reservoir with a gas cap in TMG-01 and TMG-05A Fig. 4.3 and bypassed reservoir C is an oil reservoir without a gas cap TMG-01 (Fig.11). (Fig.12) illustrates the distribution of hydrocarbon fluid in major reservoir sand B in wells TMG 02, TMG 05A, and TMG 03. Gas is the only hydrocarbon fluid within the Sand B Reservoir.

In major Sand B, water was encountered in TMG-02 (1548 m), a shallower depth than the depth at which gas was discovered in TMG-05A (1565 m), (Fig. 12); these would imply against the law of physics that water overlies gas within

the same reservoir, which is an illogical apparent density inversion. The correct situation is that the reservoir is faulted between TMG 02 and TMG 05, with TMG 02 located in the upthrown block. The fault acts as a sealing fault that prevents fluids from migrating between TMG 02 and TMG 05 well sites. (Fig.12) shows hydrocarbon fluid distribution within major reservoir sand B in wells TMG 01, TMG 02, TMG 05A, and TMG 03.

03. Only water occurs within the Reservoir at TMG 01. The reservoir is water-filled at TMG 01 at a shallower depth (1550 m), while it is gas and oil-bearing at deeper depths of 2220 m, 2280m, 2200 m, respectively in TMG 02, TMG 05A, and TMG 03. These imply that a sealing fault placed the reservoir on its upthrown block at TMG 01 site, while TMG 02, TMG05A, and TMG-03 are on its downthrown block. This fault was earlier captured in (Fig.9). Fluid distribution within major reservoir D, (Fig.13).

In major Sand D, Gas, oil, and water occur within the Reservoir in TMG 02, TMG 05A, and TMG

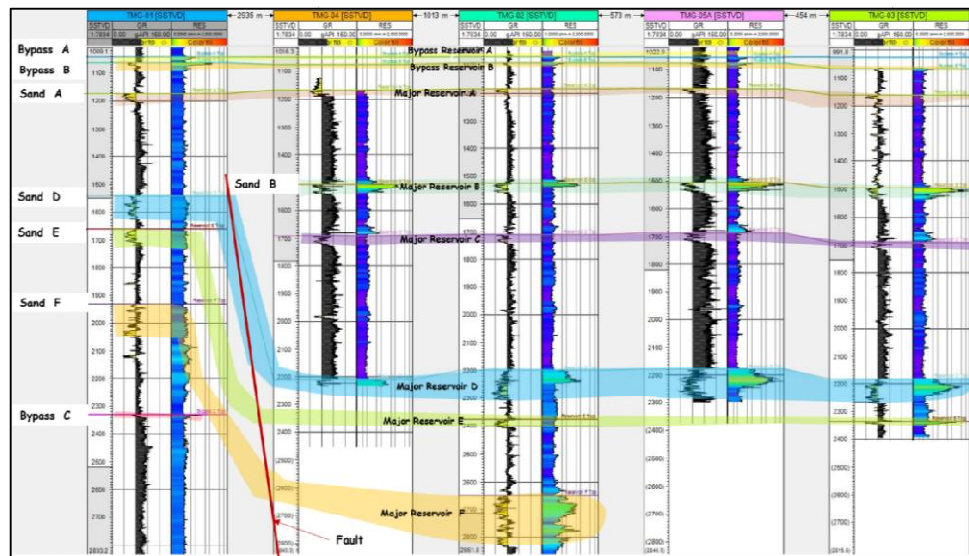


Fig. 9. Reservoir Correlation of the Major and Identified bypassed Reservoirs

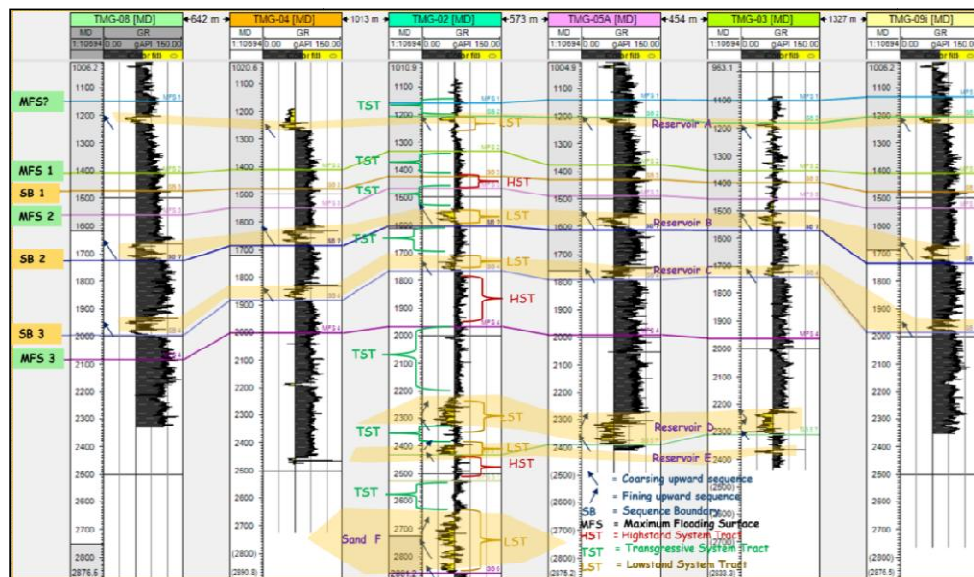


Fig.10. The Correlated sequence stratigraphic framework for the wells in Okpela Field

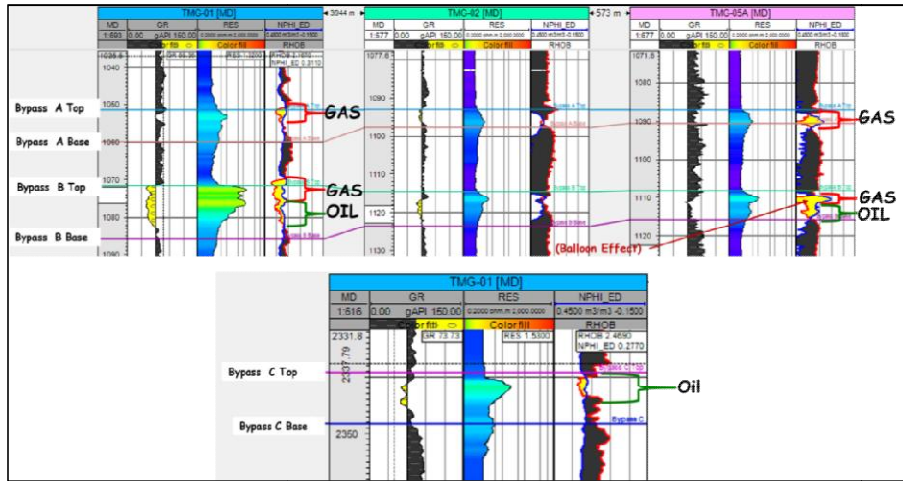


Fig. 11. Hydrocarbon fluid distribution correlation in bypassed reservoir zones in wells TMG-01, TMG-02, and TMG-05A

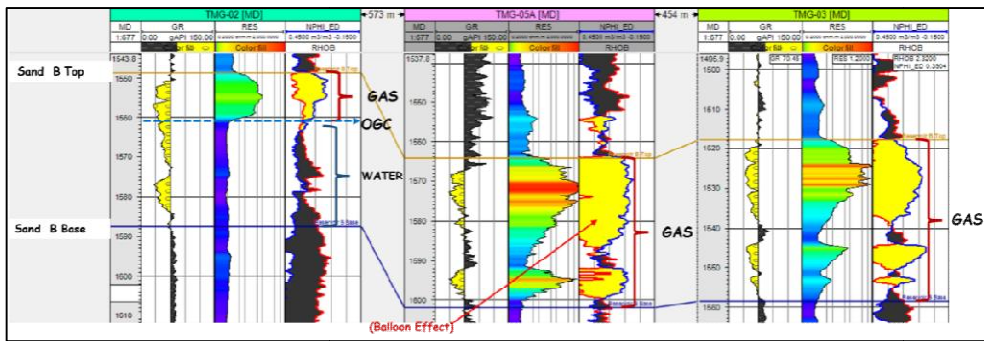


Fig.12. Hydrocarbon fluid distribution correlation in Major Reservoir Sand B in Well TMG-02, TMG-05A, and TMG-03

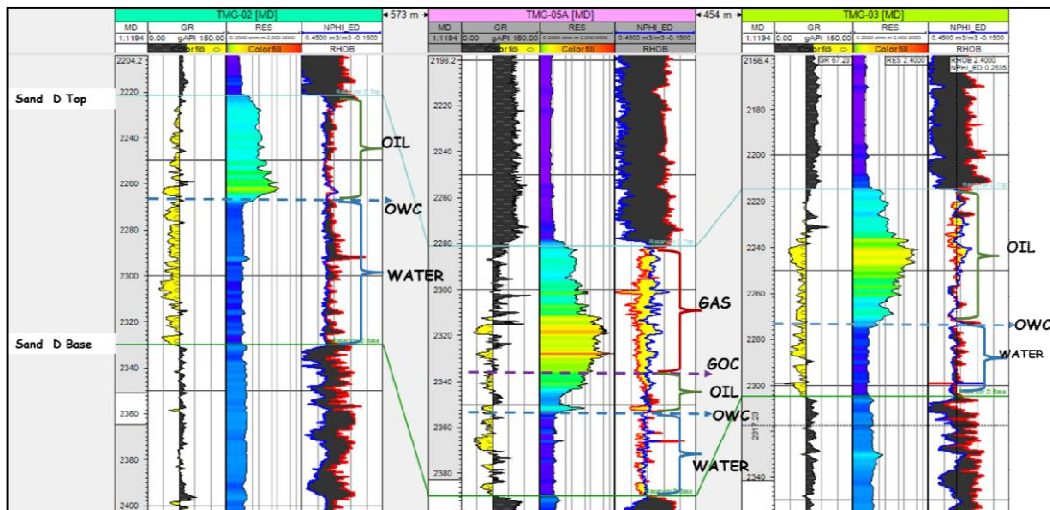


Fig. 13. Hydrocarbon fluid distribution correlation within the Major Reservoir Sand D in Well TMG-02, TMG-05A, and TMG-03

The fluid type within Sand E is gas as identified on well TMG-03. Sand E in well TMG-01 and TMG-02 is water-filled, (Fig.14). The fluid type in major reservoir Sand F in well TMG-02 is Condensate (Fig.15). The Sand F is compartmentalized from water-bearing in its up-thrown block, penetrated by TMG-01 due to the subsurface structure like faulting. The gas and oil contact could not be established because of uncertainties in the gas and oil-water contact due to high temperature and pressure in the reservoir, as provided by the engineering report.

The identified hydrocarbon-bearing reservoir was plotted and evaluated within each well to know the petrophysical properties of the reservoirs across each well. Empirical formulae [31].

were used to estimate the petrophysical properties of the correlated reservoir units delineated from the Well logs. The reservoir units, which were identified using gamma-ray and resistivity curves, were further characterized quantitatively to arrive at the following parameters: Volume of shale, porosity, hydrocarbon saturation, water saturation, gross thickness, net thickness, which are represented as figures in the petrophysical plot. The petrophysical properties of each reservoir were also characterized according to their pay zone properties which are presented using tables [32].

4.4 Petrophysical Evaluation Analysis

Shale volume (V_{CL}), porosity (Φ), water saturation (S_w), hydrocarbon saturation (S_h), gross reservoir thickness, and net pay thickness are the petrophysical parameters estimated for reservoirs in wells TMG 01, TMG 02, TMG 03, and TMG 05A.

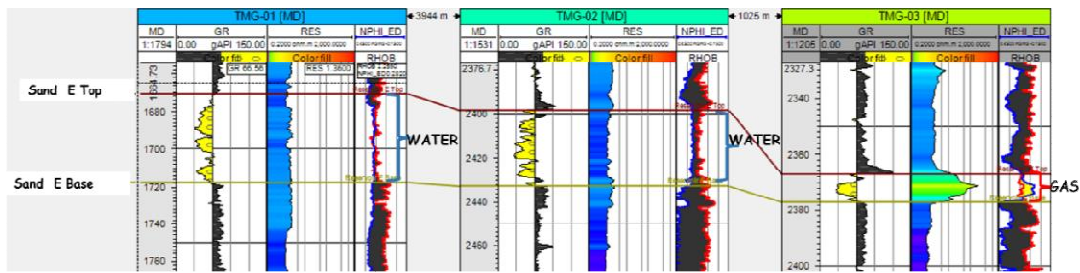


Fig. 14. Fluid distribution correlation within the Major reservoir Sand E in Wells TMG-01, TMG-02, and TMG-03

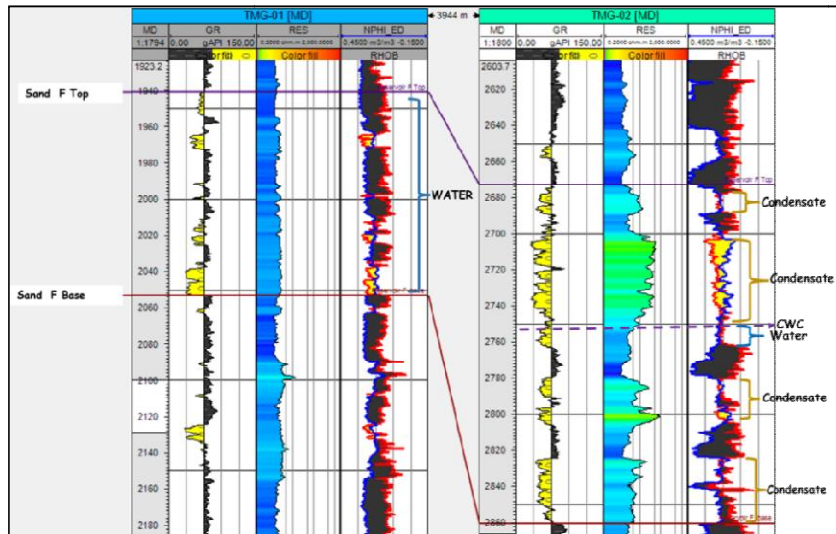


Fig.15. Fluid distribution correlation within major reservoir Sand F in wells TMG-01 and TMG-02

4.5 Petrophysical Properties Estimated for TMG-01

The petrophysical properties estimated for bypassed reservoirs in TMG 01 are presented in (Fig.16) and Table 1. Bypassed A has a net pay of about 3 m, Bypass B is about 10m, and Bypass C is about 3 m. Bypass A's hydrocarbon saturation is about 72%, GWC is -1049 m, Bypass B's hydrocarbon saturation is about 73%, GOC is -1071 m, and OWC is about -1075 m, and hydrocarbon saturation of Bypass C is about 77%, with an OWC of -2337 m. The lowest known Gas contact or oil contact is taken as the gas-water contact and oil-water contact, respectively.

4.6 Petrophysical Properties Estimated for TMG-02

Bypass A has gas, and Bypass B has oil in Well TMG-02. (Fig.17). From the pay zone petrophysical analysis of Table 2, it can be observed that the net pay of the Bypass A is about 1.22 m, Bypass B is about 3.7 m. Hydrocarbon saturation of Bypass A is about 75%, GWC is -1074 m, hydrocarbon saturation of Bypass B is about 73%, and OWC is -1100 m. The major Reservoirs such as Sand B have net pay of 12.8 m, hydrocarbon saturation of 76%, and GWC of -1538 m. (Fig.18). Sand C has net pay of 2.13 m, hydrocarbon saturation of about 32%, and GWC of -168 4 m. Sand D has net pay of 43 m, hydrocarbon saturation of 60%, GWC of

-2206 m, and OWC of -2245 m; the gas oil-water separation is represented in the evaluation plot (Fig.19). Sand F is subdivided into F1, F2, F3, F4, and F5 to avoid shale intercalation within the reservoir. Sand F1 to F5 has hydrocarbon saturation of 35%, 50%, 70%, 58%, and 40%, respectively, with net pay of 0.61 m, 10.36 m, 50.29 m, 19.2 m and 21.3 m, respectively (Fig.20).

4.7 Petrophysical Properties Estimated for TMG-03

The petrophysical properties estimated for TMG 03 are presented in Table 3. The petrophysical plots and analysis of TMG-03 are presented in (Figs.21, 22 and 23). Bypass B is the only encountered bypass zone in TMG -03, which has gas. From the pay zone petrophysical analysis Table 3, the net pay of Bypass B is about 1.8 m, hydrocarbon saturation of Bypass B is about 63%, and GWC is -1075. The major Reservoir, Sand B, has net pay of 24.38 m, hydrocarbon saturation of about 70%, and GWC of -1538 m. Sand C, which is subdivided into C1 and C2 to account for the shale intercalation, has net pay of 3 m and 14.63 m, hydrocarbon saturation of about 40% and 42%, and GWC of -1658 m and -1685 m, respectively. Sand D has net pay of 58 m, hydrocarbon saturation of about 77% and GWC of -2215 m, and OWC of -2245 m; the gas oil-water separation is represented in the evaluation plot (Fig.23).

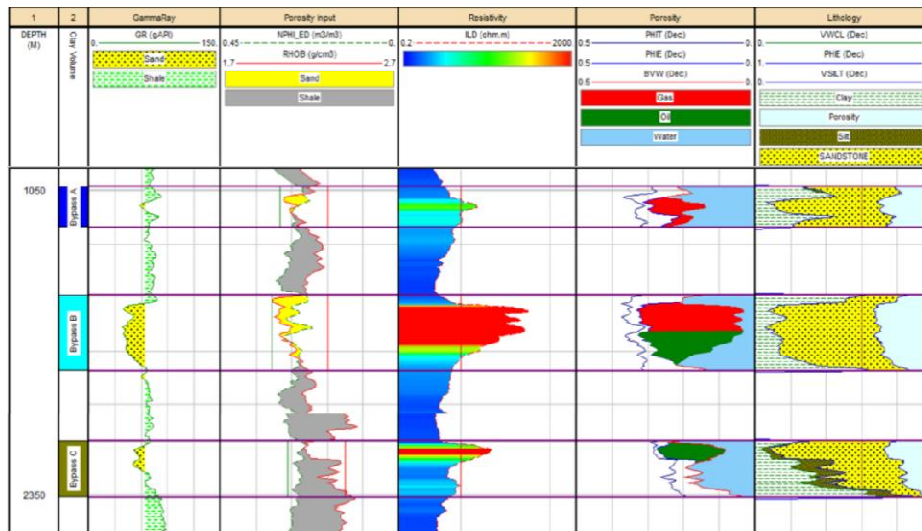


Fig. 16. Petrophysical plot of TMG-01 showing the fluid in the Bypassed reservoirs in which Bypass A is gas, Bypass B is oil and gas, and Bypass C is oil

Table 1. Petrophysical properties estimated for bypassed reservoirs in TMG-01

Zone Name	Top (sstvd)(m)	Base (sstvd)(m)	Gross	N/G	Net pay	Av vcl	Av Phi	Av Sw	Av Sh	Contact	Fluid
Bypass A	1041	1049	7.62	3.05	0.4	0.147	0.287	0.619	0.381	-1049	GAS
Bypass B (gas)	1061	1071	8.1	6	0.717	0.13	0.27	0.269	0.731	-1071	GAS
Bypass B (oil)	1071	1075	6.3	4.01	0.7	0.13	0.23	0.251	0.722	-1075	OIL
Bypass C	2330	2340	10.67	3.05	0.286	0.085	0.26	0.416	0.584	-2337	OIL

Table 2. Petrophysical properties estimated for the major and bypassed reservoirs in TMG-02

Zone Name	Top (sstvd)(m)	Base (sstvd)(m)	Gross	N/G	Net pay	Av vcl	Av Phi	Av Sw	Av Sh	Contact	Fluid
Bypass A	1069	1074	5.18	1.22	0.235	0.297	0.26	0.694	0.306	-1074	Gas
Bypass B	1091	1100	5.79	3.66	0.632	0.259	0.22	0.677	0.323	-1100	OIL
Sand B	1515	1538	23.16	12.8	0.553	0.159	0.209	0.241	0.759	-1538	Gas
Sand C	1680	1685	5	2.13	0.426	0.214	0.201	0.682	0.318	-1684	Gas
Sand D (gas)	2198	2206	7.62	5.03	0.66	0.222	0.249	0.504	0.496	-2206	Gas
Sand D (oil)	2206	2245	38.71	37.95	0.98	0.223	0.267	0.339	0.661	-2245	Gas
Sand F1	2620	2637	16.46	0.61	0.037	0.077	0.221	0.647	0.353	-2635	Condensate
Sand F2	2651	2665	14.63	10.36	0.708	0.11	0.235	0.497	0.503	-2665	Condensate
Sand F3	2676	2732	56.08	50.29	0.897	0.156	0.232	0.308	0.692	-2729	Condensate
Sand F4	2755	2782	26.52	19.2	0.724	0.153	0.22	0.42	0.58	-2782	Condensate
Sand F5	2801	2836	35.97	21.03	0.585	0.144	0.229	0.598	0.402	-2836	Condensate

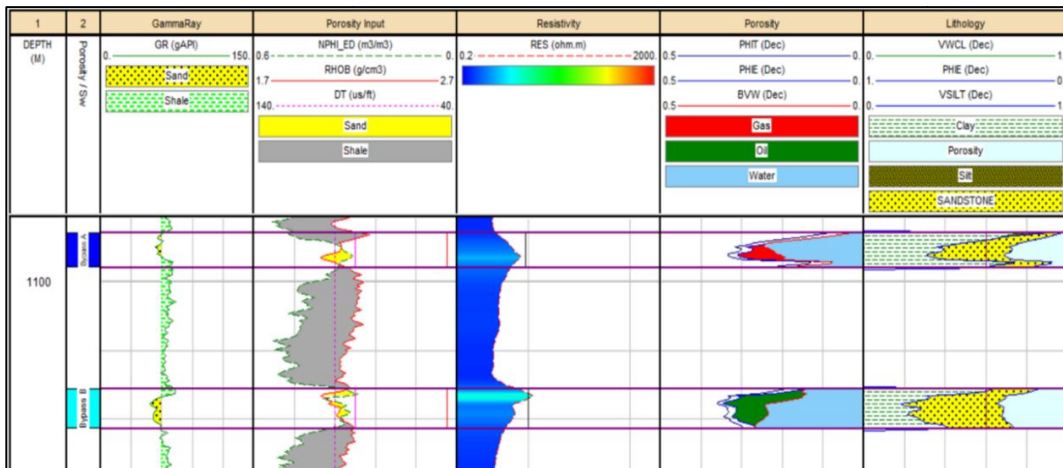


Fig. 17. Petrophysical plot of TMG-02 showing the fluid in Bypass A and B

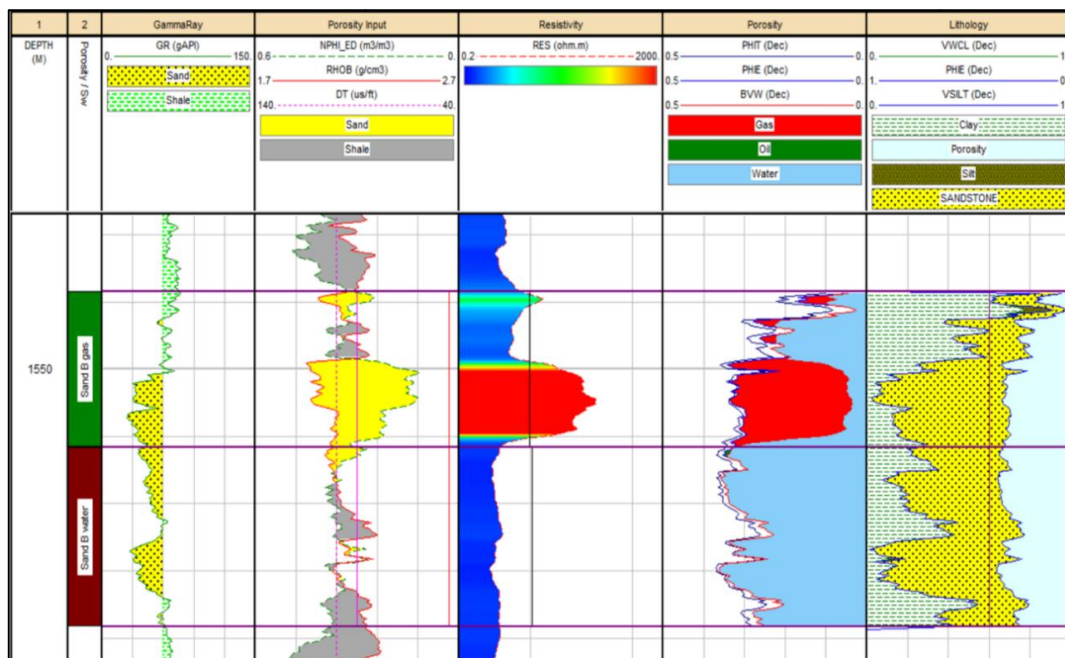


Fig. 18. Petrophysical Plot of TMG-02 showing the Sand as Gas

4.8 Petrophysical Properties Estimated for TMG-05A

(Figs.24, 25, 26 and 27) show the petrophysical plots of TMG-05A. Table 4 shows the petrophysical properties estimated for each reservoir. Bypass A and B have gas in well TMG-05A (Fig.24), from the pay zone petrophysical analysis Table 4, It can be observed that the net pay of the Bypass A is about 4.65 m, Bypass B is about 5m.

Hydrocarbon saturation of Bypass A is about 65%, GWC is -1060 m, hydrocarbon saturation of Bypass B is about 68%, and GWC is -1082 m. The major Reservoirs such as Sand B have net pay of 39.17 m, hydrocarbon saturation of 75%, and GWC of -1538 m. Sand C has net pay of 16.15 m, hydrocarbon saturation of 43%, GWC of -1685 m, and Sand D has net pay of 64 m, hydrocarbon saturation of 84%, GWC of -2219 m, and OWC of -2245 m; the gas oil-water separation is represented in the evaluation plot.

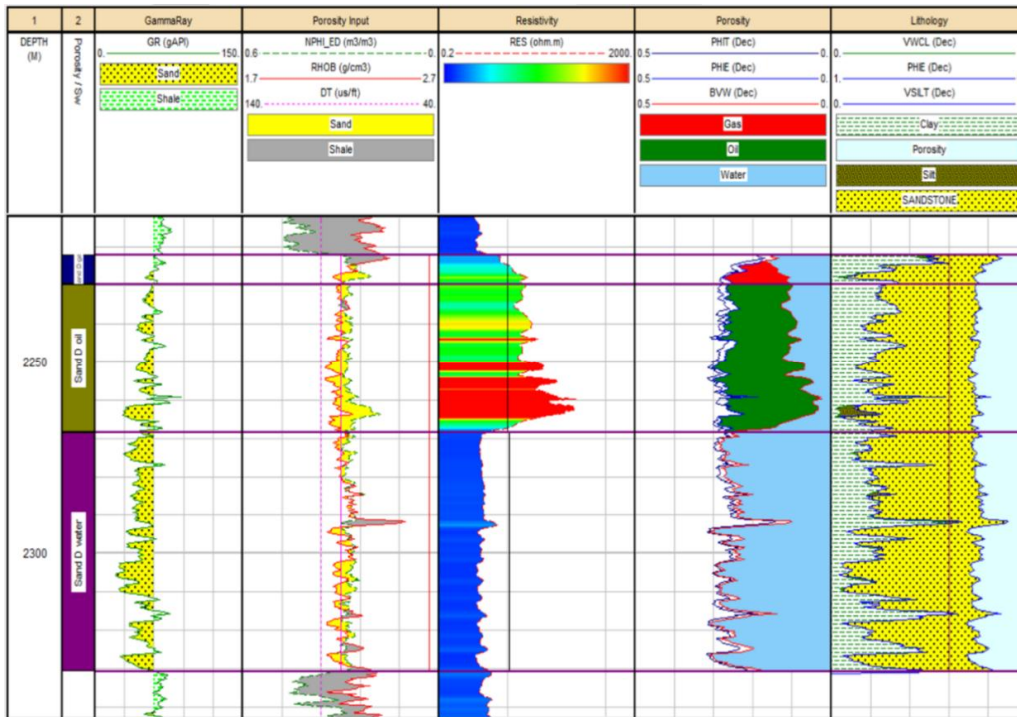


Fig. 19. Petrophysical Plot of TMG-02 showing the fluid in Sand D as having oil with a gas cap

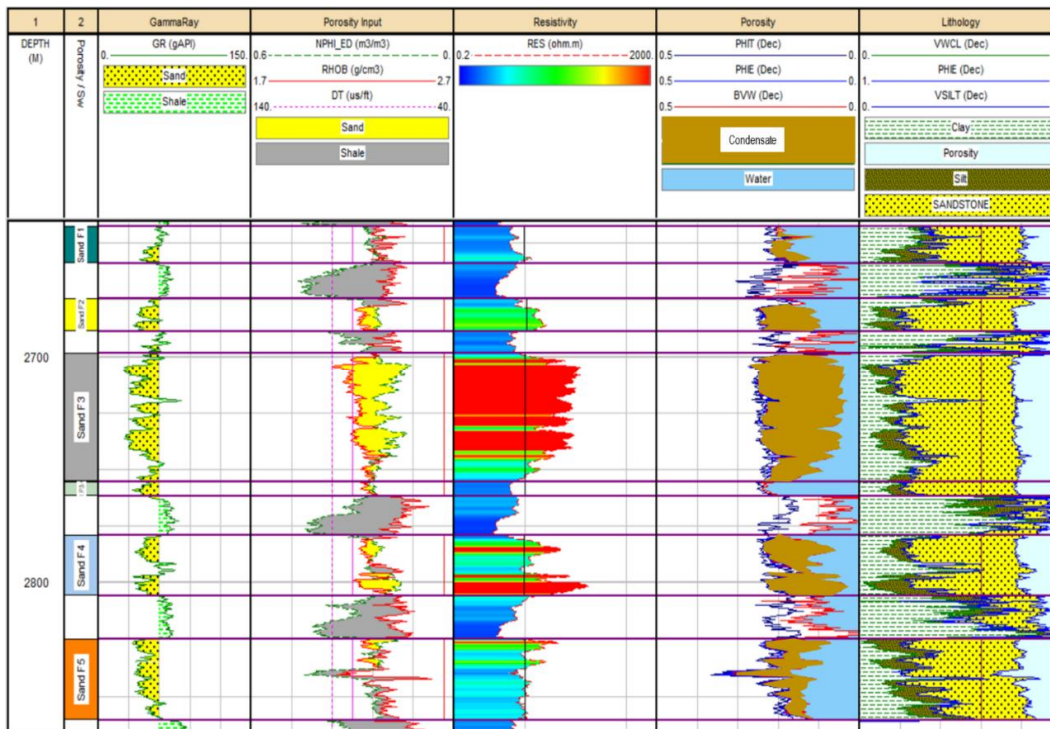


Fig. 20. Petrophysical plot of TMG-02 showing the Gas condensate saturation within the Sand F subdivided reservoir

Table 3. Petrophysical properties estimated for major and bypassed reservoirs in Well TMG-03

Zone Name	Top (sstvd)(m)	Base (sstvd)(m)	Gross	N/G	Net pay	Av vcl	Av Phi	Av Sw	Av Sh	Contact	Fluid
Bypass B	1066	1075	7.92	1.83	0.231	0.102	0.212	0.682	0.318	-1075	GAS
Sand B	1494	1536	40.23	24.38	0.606	0.13	0.281	0.314	0.686	-1536	GAS
Sand C1	1653	1658	14.02	3.05	0.217	0.133	0.199	0.629	0.371	-1658	GAS
Sand C2	1664	1685	19.51	14.63	0.75	0.152	0.214	0.578	0.422	-1685	GAS
Sand D (gas)	2182	2203	19.51	18.75	0.961	0.15	0.255	0.433	0.567	-2215	GAS
Sand D (oil)	2203	2245	71.63	39.17	0.547	0.107	0.272	0.232	0.768	-2245	OIL
Sand E	2335	2345	11.28	6.4	0.568	0.196	0.22	0.273	0.727	-2345	GAS

Table 4. Petrophysical properties estimated for major and bypassed reservoirs in Well TMG-05A

Zone Name	Top (sstvd)(m)	Base (sstvd)(m)	Gross	N/G	Net pay	Av vcl	Av Phi	Av Sw	Av Sh	Contact	Fluid
Bypass A	1055	1060	5.18	4.65	0.897	0.219	0.231	0.6	0.4	-1060	GAS
Bypass B	1075	1082	7.32	4.88	0.667	0.2	0.275	0.593	0.407	-1082	GAS
Sand B	1494	1542	53.8	39.17	0.728	0.153	0.289	0.253	0.747	-1536	GAS
Sand C1	1658	1664	10.67	2.74	0.257	0.169	0.268	0.58	0.42	-1664	GAS
Sand C2	1668	1685	18.14	13.41	0.739	0.125	0.229	0.556	0.444	-1685	GAS
Sand D gas	2178	2206	29.72	28.12	0.946	0.205	0.259	0.313	0.687	-2219	GAS
Sand D oil	2206	2246	42.06	35.89	0.853	0.114	0.272	0.16	0.84	-2245	OIL

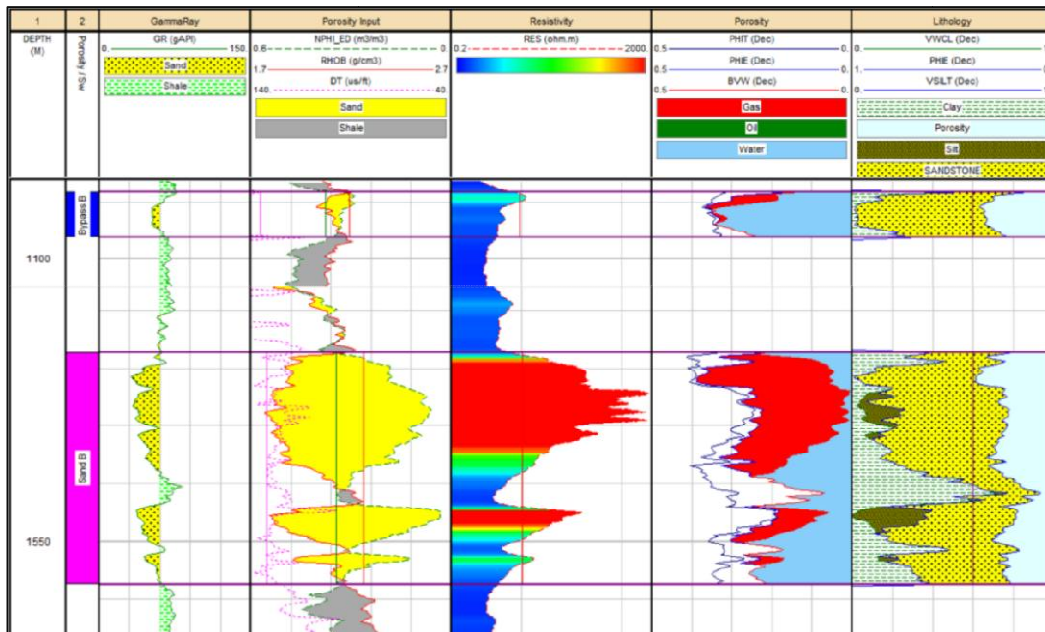


Fig. 21. Petrophysical plot of TMG-03 showing the hydrocarbon in Bypass B as gas and Sand B as gas

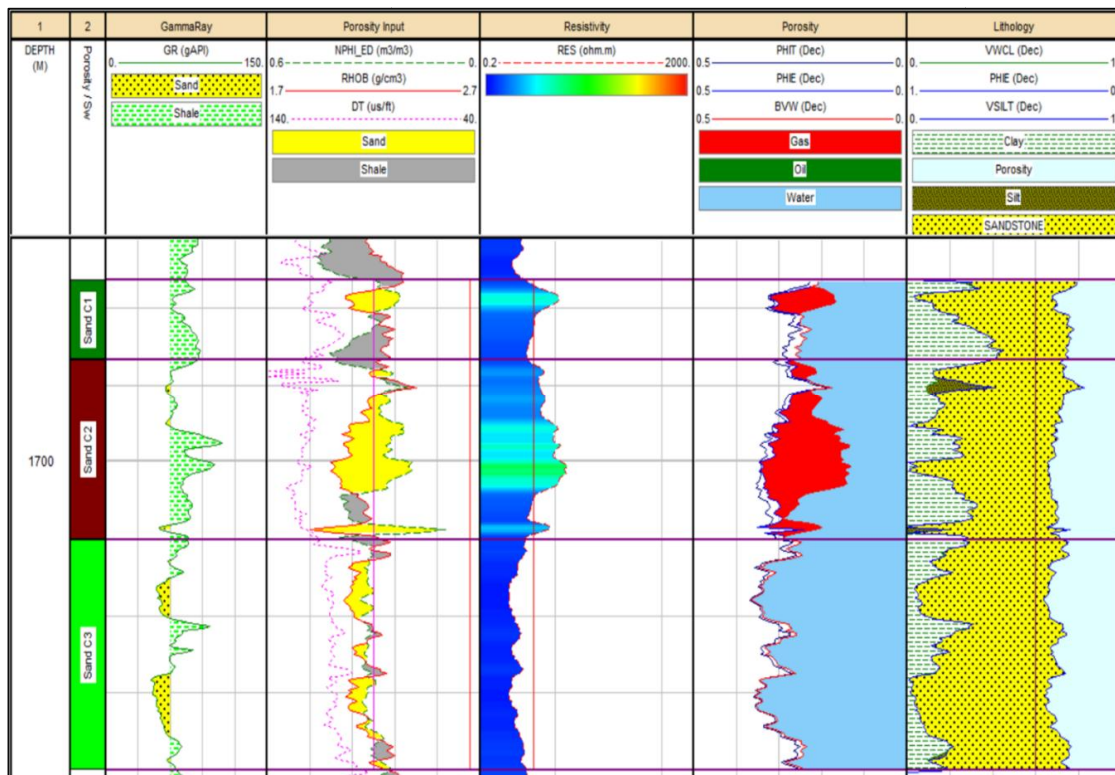


Fig. 22. Petrophysical plot of TMG-03 showing the hydrocarbon in Sand C as gas

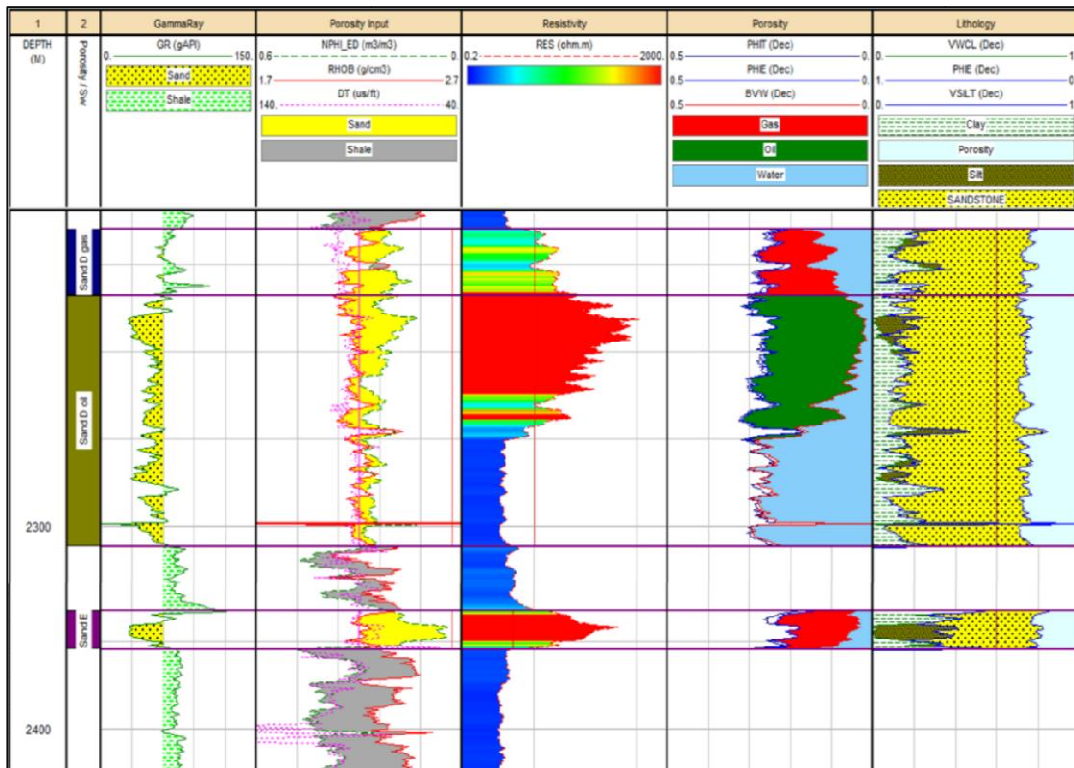


Fig. 23. Petrophysical Plot of TMG-03 showing the hydrocarbon in Sand D as oil with gas gap and Sand E as gas

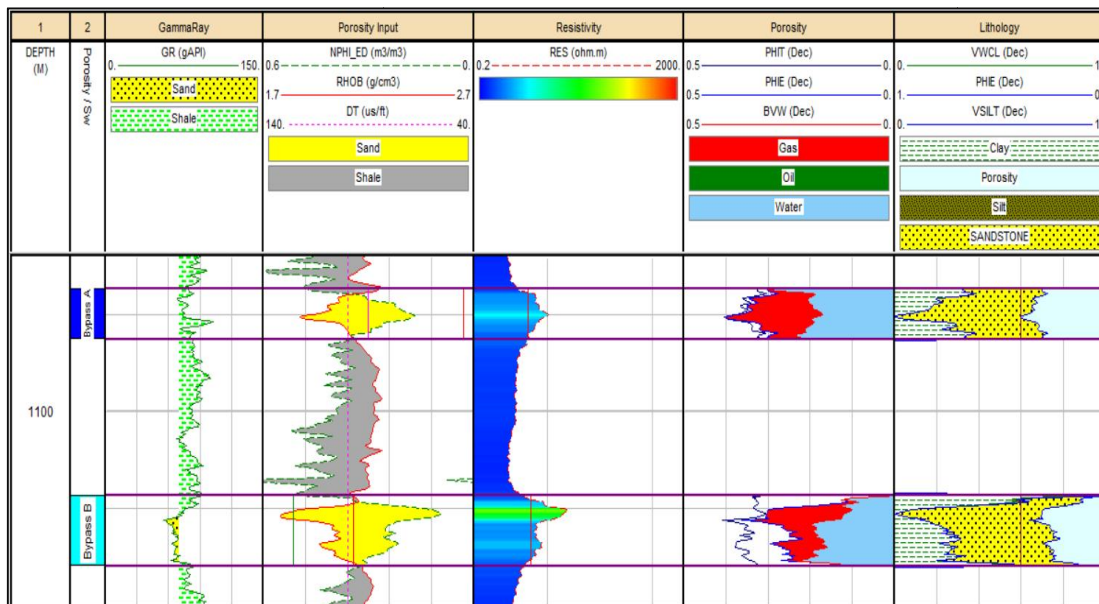


Fig. 24. Petrophysical Plot of TMG-05A showing the hydrocarbon in Bypass A and B as gas

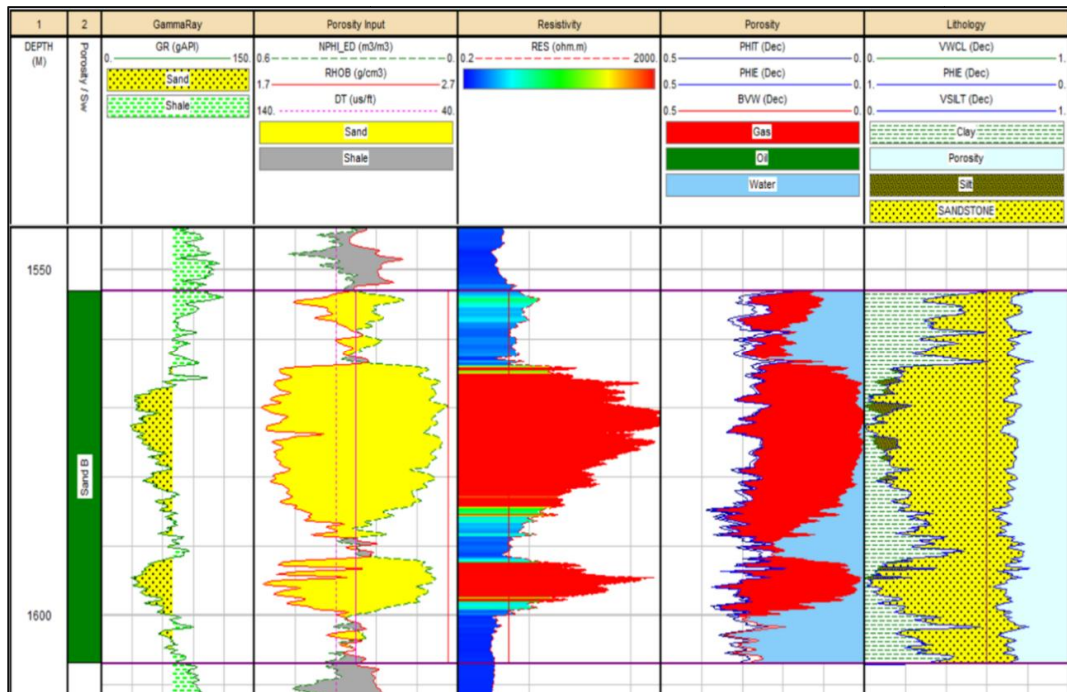


Fig. 25. Petrophysical plot of TMG-05A showing the fluid in Sand B as Gas

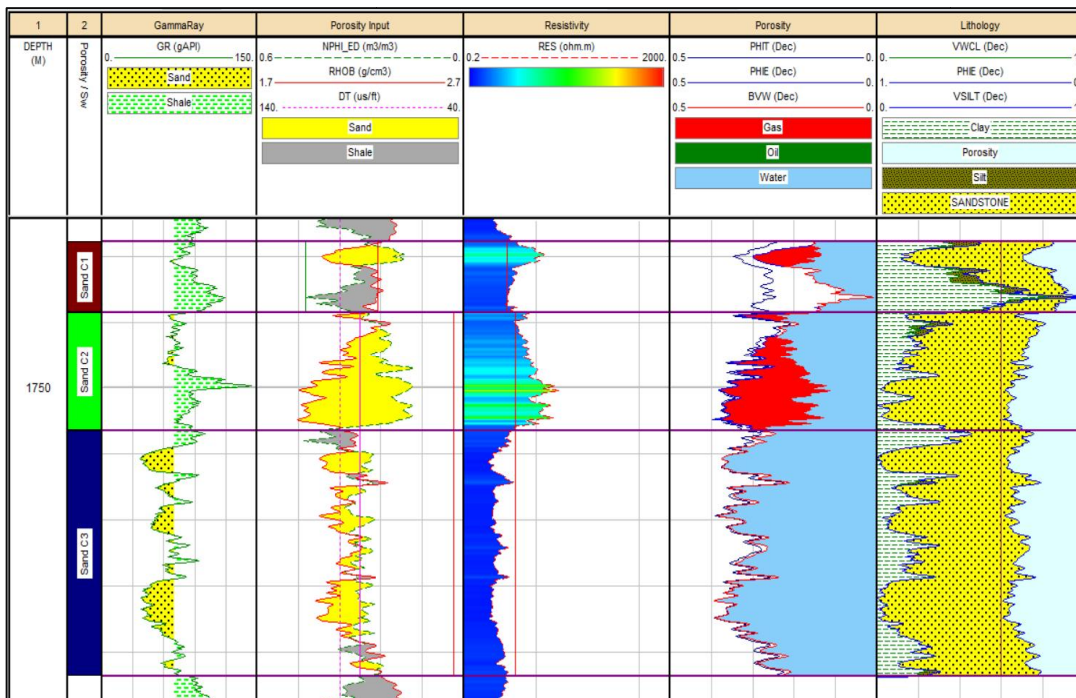


Fig. 26. Petrophysical plot of TMG-05A showing the hydrocarbon in Sand C as Gas

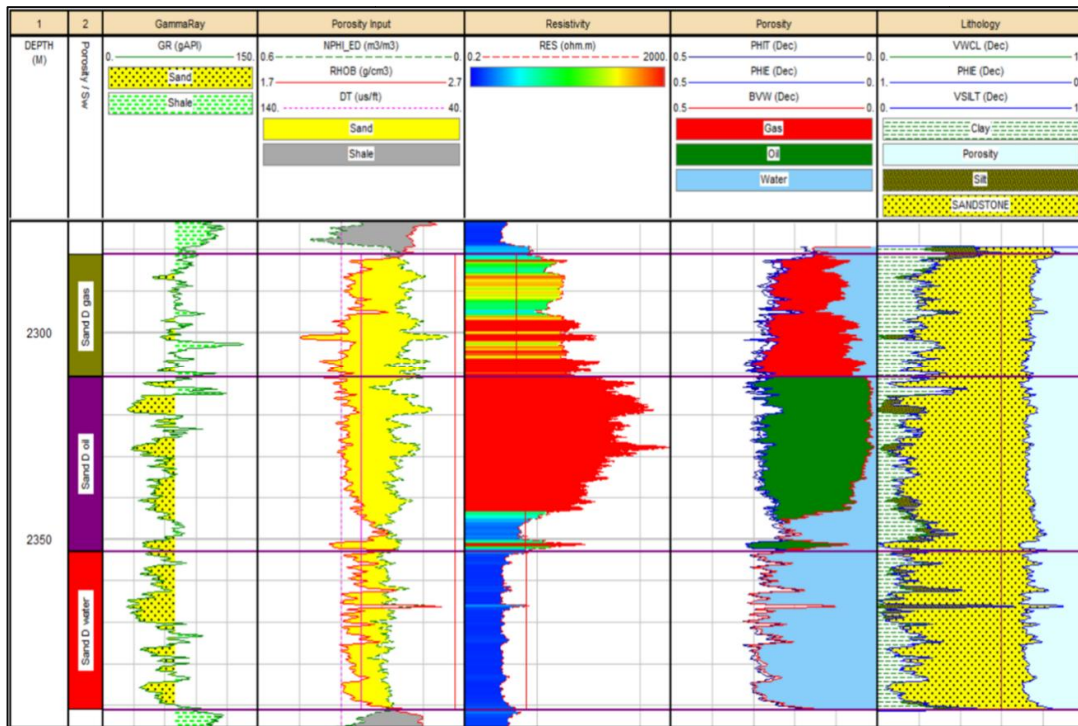


Fig. 27. Petrophysical plot of TMG-05A showing the hydrocarbon in Sand D as oil with a gas cap

5. CONCLUSION

The Well-log analysis revealed that the subsurface geology is composed of Sand and shale intercalations. The Sand acts as a reservoir for hydrocarbon accumulation within the Okpila Field Offshore Niger Delta Basin. The reservoirs were correlated across the wells where six major Reservoirs and three Bypass Reservoirs were identified. The major Reservoirs are the reservoirs identified by the operating company that provided the data. The identified Bypass Reservoirs within the context of this study will enhance the Field's future development. The major reservoirs are Sand A, B, C, D, E, and F, while the Bypass Reservoirs are Bypass A, B, and C.

The biostratigraphic data were used in the research to achieve the sequence stratigraphic correlation. These revealed that the Reservoirs within study area lie within the Low stand System tract (LST). The depositional environment was interpreted to be shoreface deposit. The reservoirs were deposited during the Pliocene and Miocene. The stacking pattern of the gamma-ray log motif and the stratigraphic

data were integrated to generate this interpretation.

In conclusion, this study was able to identify three additional reservoirs, called Bypass reservoirs for simplicity. These bypass reservoirs contain gas, oil, or both, and with appreciable petrophysical properties. Exploiting this additional bypassed reservoir can add to the production life of the Field.

COMPETING INTERESTS

Authors have declared that no competing interests exist.

REFERENCES

1. Ekwe AC, Onuoha KM. Using rock physics modelling and Lambda Murho inversion to enhance exploration in a mature producing field in the onshore Niger Delta basin. In K. M. Onuoha, ed) *Advances in Petroleum Geoscience Research in Nigeria (Basin). Analysis and Reservoir Characterisation Studies* University of Nigeria, Nsukka: Published by PTDf. 2017;1-18.

2. Slatt RM. Stratigraphic reservoir characterization for petroleum geologists, geophysicists and engineers. Elsevier, Amsterdam. 2006;473.
3. Ahmed H. Senosy, Hatem F. Ewida, Hassan A. Soliman, and Mohamed O. Ebraheem. Petrophysical analysis of well logs data for identification and characterization of the main Reservoir of Al Baraka Oil Field, Komombo Basin, Upper Egypt. Springer Nature Applied Science. 2020;2:1293.
4. Lyaka AL, Mulibo GD. Petrophysical analysis of the Mpapai well logs in the east Pande exploration block, southern coast of Tanzania: geological implication on the hydrocarbon potential. Open J Geol. 2018;8:781-802.
5. Ologe O. Reservoir evaluation of "T-X" field (Onshore, Niger Delta) from well log and petrophysical analysis. Bayero J. Pure & Appl. Sci. 2016;9(2):132-140.
6. Maju-Oyovwikowhe GE, Njoku, Vk. Petrophysical Analysis of Well Logs for Reservoir Evaluation: A Case Study of Well 1 and 2 of the 'Ictorian' Field in the Niger Delta Basin. J. Appl. Sci. Environ. Manage. 2019;23(6):999-1006.
7. Mohamed Mahmoud Elhossainy, Ahmed Kamal Basal, Hussein Tawfik ElBadrawy, Sobhy Abdel Salam and Mohammad Abdelfattah Sarhan. Well, logging data interpretation for appraising the performance of Alam El-Bueib reservoir in Safir Oil Field, Shushan Basin, Egypt. Journal of Petroleum Exploration and Production Technology. 2021;11:2075-2089.
8. Rotimi O, Adeboye T, Ologe O. Petrophysical Analysis and Sequence Stratigraphic Appraisal from Well logs of 'Bobo' Field, South-Eastern, Niger Delta. Journal of Emerging Trends in Engineering and Applied Sciences (JETEAS). 2013;4(2):219-225.
9. Obaje N. Sequence Stratigraphic Interpretation of Kafe-1 Field, Offshore Western Niger Delta. International Journal of Engineering Science Invention. 2009;2.
10. Kulke H. In Kulke, H. (Ed.), Nigeria, Regional petroleum geology of the world. Part II: Africa, America, Australia and Antarctica. Berlin, Gebruder Borntraeger. 1995;143-172.
11. Hospers J. Gravity field and structure of the Niger Delta, Nigeria. West Africa. GSA Bulletin. 1965;74(1):1-12.
12. Weber KJ, Daukoru EM. Petroleum Geology of the Niger Delta. Proceedings of the Ninth World Congress held in London, United Kingdom. 1975;10-17.
13. Evamy, et al. Hydrocarbon Habitat of Tertiary Niger Delta. American Association of Petroleum Geologists Bulletin. 1978;62:1-39.
14. Doust HJ, Omatsola E. Niger Delta in Edwards, J. D. and Santoyiossi, P.A. (Ed.); 1990.
15. Shannon PM, Naylor N. Petroleum Basin Studies. London, UK: Graham and Trotman Limited. 1989;153-169.
16. Doust HJ, Omatsola E. Niger Delta. American Association of Petroleum Geologist Bulletin. 1989;48:201-238.
17. Whiteman AJ. Nigeria: Its petroleum geology, resources and potentials. London, U.K.: Graham and Trotman. 1982;170-282.
18. Short KC, Stauble AJ. Outline of Geology of Niger Delta. AAPG Bulletin. 1967;51(1):761 – 779.
19. Catuneanu D. Principles of Sequence Stratigraphy. AE Amsterdam: Elsevier Radarweg Publishing; 2006.
20. Emery D, Myers KJ. sequence stratigraphy. Blackwell Science Limited. 2006;297.
21. Ola-Buraimo AO, Ogala JE, Adebayo OF. Well-Log Sequence Stratigraphy and Paleobathymetry of Well-X, Offshore Western Niger Delta, Nigeria. World Applied Sciences Journal. 2010;10 (3): 330-336.
22. Amigun JO, Odole OA. Petrophysical properties evaluation for reservoir characterization of Seyi oil field (Niger-Delta). Int J Innov Appl Stud. 2013;3:765-773.
23. Larionov V. Borehole Radiometry. Moscow, Soviet Union.: National Electric Drag Racing Association; 1969.
24. Islam A, Habib M, Islam M, Mita M. Interpretation of wireline log data for reservoir characterization of the Rashidpur GasField, Bengal Basin. . Bangladesh. 2013;1:47-54.
25. Bowen D. Formation Evaluation and Petrophysics. Indonesia: Core Laboratories, Jakarta. 2003;273.
26. Nwankwo C, Anyanwu J, Ugwu S. Integrating seismic and well log data for

- petrophysical modelling of sandstone hydrocarbon reservoir in Niger Delta. *Scientia Africana*. 2014;13:186-199.
27. Khayer K, Shirazy A, Shirazi A, Ansari A, Nazerian H, Hezarkhani A. Determination of Archie's Tortuosity Factor from Stoneley Waves in Carbonate Reservoirs. *International Journal of Science and Engineering Applications*. 2021;10(08): 107-110.
28. Pickett GR. *Practical formation evaluation*. Golden Colorado: G. R. Pickett, Inc; 17972.
29. Crain E. Visual analysis rule for water saturation. Retrieved from *Petrophysical Handout*; 2019. Available: <https://www.spec2000.net/14-swbasics.htm>
30. Darwin VE, Singer JM. *Well Logging for Earth Scientists* 2nd Edition. Buisness Media B.V: Springer; 2008.
31. Archie G. The electrical resistivity log as an aid in determining some reservoir characteristics. . *Trans AIME*.146:54-62.
32. *Divergent and Passive Margin Basin*. AAPG Memoir. 1942;48:201 – 238.

© 2022 Waziri et al.; This is an Open Access article distributed under the terms of the Creative Commons Attribution License (<http://creativecommons.org/licenses/by/4.0>), which permits unrestricted use, distribution, and reproduction in any medium, provided the original work is properly cited.

Peer-review history:
The peer review history for this paper can be accessed here:
<https://www.sdiarticle5.com/review-history/84946>